Mat. Res. Soc. Symp. Proc. Vol. 758 © 2003 Materials Research Society LL4.6

Two-Photon Laser Micro-Nano Fabrication; Understanding from Single-Voxel Level

Satoshi Kawata[1] and Hong-Bo Sun[2]
Department of Applied Physics, Osaka University, Suita, Osaka, 565-0871, Japan
[1]The Institute of Physical and Chemical Research (RIKEN), Hirosawa, Wako, Saitama 351-0198, Japan
[2]PRESTO, Japan Science and Technology Corporation (JST)

ABSTRACT

For laser nanofabrication using two-photon photopolymerization, a deep understanding of the nature of focal spots that are related to two-photon excitation is essential for achieving a high spatial resolution in three dimensions. Here we report the use of a technology we call ascending scan for characterizing the three-dimensional size and shape of single polymerization elements (voxels), and introduce several features of voxels that have not been fully noticed before. These findings are important for tailoring nanofeatures according to design.

INTRODUCTION

Two-photon photopolymerization [1-7] has been recognized as an important technology for nanofabrication. The current research effort is mainly devoted to the synthesis of high efficiency photo initiators and sensitizers [4, 10]. However, as a new technology, a lot of work has been done to establish it as a nanotechnology. Examples include the achievement of sub-diffraction-limit spatial resolution by the radical quenching effect [8, 9], improvement of fabrication efficiency by using 3D vector scanning [9], 3D micro-diagnosis by fluorescent dye labeling and two-photon confocal scanning [11], micro-device functionalization [12], and so forth. Different from conventional laser rapid prototyping, depicting micro-objects with SDL features needs a deep understanding of characteristics of two-photon excitation related focal spots. This work has not been done before. In this paper, we will introduce a 3D focal spot imaging technology, ascending scan [13], and an investigation by using this technology on how basic laser parameters influence the focal spot size and shape, and therefore the nanofabrication.

EXPERIMENTAL SYSTEM

The experimental system was the same as we used before [12, 13]. A Ti: Sapphire laser that was operated at mode-lock and delivered 100 fs pulses at a repetition rate of 80 MHz was

employed as an exposure source (MaiTai, Spectra Physics). The laser wavelength was tuned to 780 nm. The laser beam was focused by a high-numerical-aperture (NA~1.4) objective lens into a sample. A Galvano mirror set was used for moving the focal spot in two horizontal dimensions and a piezo stage for up-down scanning, both synchronized and controlled with a computer. A urethane acrylate resin, SCR 500 (from Japan Synthetic Rubber, JSR) was used for two-photon-absorption (TPA) photopolymerization, of which the absorption peaks at UV and extends to the visible range to 530 nm. The entire fabrication process was monitored *in-situ* with a CCD camera. After fabrication, samples were developed in methanol so that unsolidified liquid was removed. Finally samples were dried and imaged with a scanning electron beam microscope.

THREE-DIMENSIONAL FOCAL SPOT CHARACTERIZATION

The 3D spatial resolution was conventionally characterized from a resin spot or line that was polymerized on the surface of a substrate. By atomic force microscope (AFM) or scanning electron microscope (SEM) measurement, the width and height of the spot were considered as the lateral and longitudinal dimensions of a voxel, in other words, the lateral and longitudinal spatial resolutions, respectively. Due to a truncation effect, the substrate surface recorded spot is actually only a part of an entire voxel. The above simple measurement scheme brought a lot of misleading conclusions. To get reliable spatial resolution information, a complete and isolated voxel is needed. To reach this end, we scan the laser focal point from inside the substrate to an above surface height, residing at a series of positions for exposure [Fig. 1(a)]. The left-side voxels are truncated, and are utilized in conventional AFM or SEM observations. In the rightmost region, voxels form but float away during developing. Only if the residing spot number is reasonably large, there are always some voxels formed at the immediate substrate surface that are not truncated and are weakly attached. After developing, these voxels remain where they were polymerized and fall down [Fig. 1(b)]. From these voxels, both lateral and longitudinal spatial resolutions are attained [Fig. 1 (c)].

VOXELS INFLUENCED BY LASER PULSE ENERGY, EXPOSURE TIME, NUMERICAL APERTURE, AND POLARIZATION

Laser beams are described by their spatial, temporal, spectral and polarization distributions in addition to coherence properties. As fundamental limits the beams can be diffraction and bandwidth limited, linearly polarized and coherent. Usually these limits are not satisfied or even required in applications.

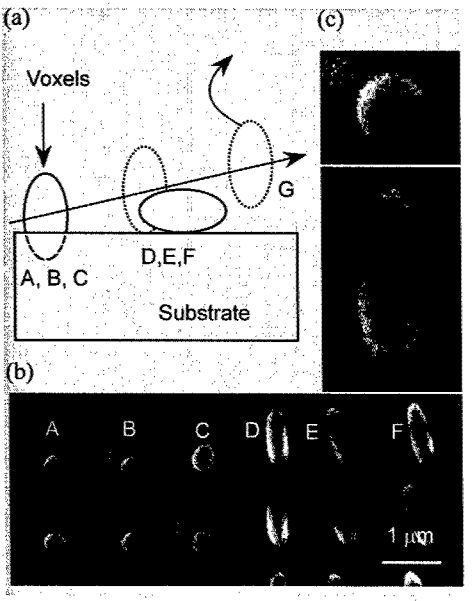

Figure 1. The ascending scan method for observation of the 3 dimensions of a voxel. (a) The principle of the technology; (b) SEM image of the truncated (A, B, C) and overturned (D, E, F) voxels; and (c) magnified images of a voxel.

In the current research, a 780-nm-wavelength laser with a 100-fs pulse width at a repetition rate of 80 MHz possesses a spectral full width at half maximum (FWHM) of approximately 10 nm, implying a time-bandwidth product of $\Delta t \cdot \Delta \omega = 0.493$, near the transform limit of 0.441 of a Gaussian pulse shape. A short pulse width (< 1 ps) is essential to provide a high transient power in time domain to launch nonlinear optical processes and exclude thermal effects, which are difficult to localize. The broad laser spectrum associated with the ultrashort pulse width brings about the chromatic aberration, which has been overcome by use of apochromats. Also due to the wide spectrum, the coherence length (l_c) of femtosecond lasers becomes short, e.g. around 40 μm in the current system as estimated by $\lambda_c = 0.624\ \lambda / \Delta\lambda_{FWHM}$, which is the major hindrance of large-volume holographic applications. For single-color and single-beam focusing geometry as we used in this research, the coherence condition for forming a virtual energy level that is needed by two-photon absorption (TPA) is naturally satisfied.

Comparing with the roles of temporal, spectral and coherence performances discussed above, laser energy distribution and beam polarization directly determine the spatial resolution of fabrication. By using the ascending method, we investigated how some basic laser parameters influence voxels, including exposure time, laser pulse energy, NA and polarization. This information is important because for tailoring nanostructures, not only the focal spot size, but also its shape determine the accuracy and dimensions of target objects.

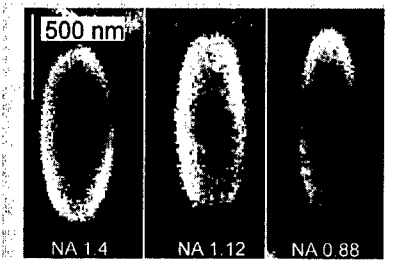

Figure 2. Side-view SEM images of voxels formed under different NA focusing.

Figure 2 shows the side-view SEM image of voxels formed under the same laser power exposure but beams focused with lens of different NAs. The longitudinal size increases as NA is reduced within expectation. However, it is found the lateral size obtained at high NA is no smaller than that at low NA. This contradicts theoretical results, but could be understood by considering the threshold effect of TPA polymerization. In case of low-NA focusing, the laser power is distributed to a larger volume, and the solidified front demarcated by the threshold camber is vertically expanded and laterally shrunk. Therefore low-NA gives smaller lateral voxel size. The gradient of light intensity distribution in high-NA focused light field is steeper and energy is more concentrated to the center of focal spot, which facilitates pinpoint exposure at smaller volume. Therefore smallest visible voxels by 1.4 and 0.8 NA are 120 nm and 260 nm, respectively. Hence, for high-accuracy nanofabrication, a high NA objective is preferable. Further research shows that near-threshold exposure condition, increasing exposure time and increasing laser pulse energy causes different exposure dose-dependent voxel size. The former is basically a logarithmic function that reflects the radical diffusion process, while the latter dependence is from an enhanced two-photon absorption effect.

We also tested how polarization influences the voxel shape. We found that the voxel cross-section perpendicular to the optical axis direction was not circular as expected, but an ellipse with axis ratio of roughly 1.1. This is shown in Fig. 3.

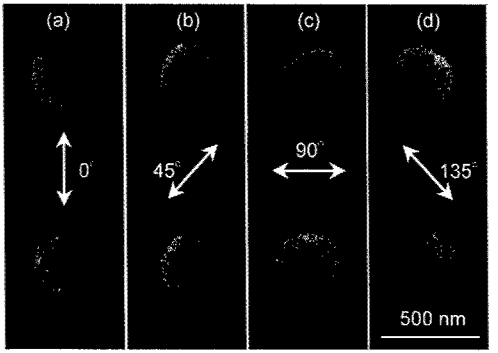

Figure 3. Top-view SEM images of voxels produced with lasers of different linear polarization directions.

The above phenomenon was explained by a depolarization effect that was predicted by electromagnetic focusing theory. It is already known that, when the beam incident angle α is small, the focal field (E_x, E_y, E_z) is sufficiently described by a cylindrically symmetric function [$E(r)$, 0,0] with $r=\sqrt{(x^2+y^2)}$, where the input beam is assumed to propagate in the z-direction and be polarized along the x-direction. Nevertheless, when $\alpha > 40^\circ$ (NA > 0.7), the symmetry is broken and the field with significant E_y and E_z component appears. More precisely, the electric field can be expressed as:

$$E(r_2,\phi,z_2)=\frac{\pi i}{\lambda}\{[I_0+\cos(2\phi)I_2]\mathbf{i}+\sin(2\phi)I_2\mathbf{j}+2i\cos\phi I_1\mathbf{k}\}$$

where **i**, **j** and **k** are the unit vectors in the x, y and z directions, respectively, variables r_2, z_2 and ϕ are cylindrical coordinates of an observation point. I_0, I_1 and I_2 are non-zero variables [see definitions in Ref.15]. Hence, it is clear that the electric field at the focal region is depolarized. The calculated result is shown in Fig. 4. The fact that the orientation of voxels changes corresponding to the polarization direction provides solid evidence for the origin of the ellipse cross-section.

CONCLUSION

We propose an ascending scan method for imaging single voxels in three dimensions. By using this technology we studied how basic laser parameters influence the shape and size of voxels. This technology and our findings are important for understanding the two-photon

photopolymerization nanofabrication technology. Also it can be utilized for evaluating newly synthesized photopolymers to test their usability in 3D laser nanofabrication.

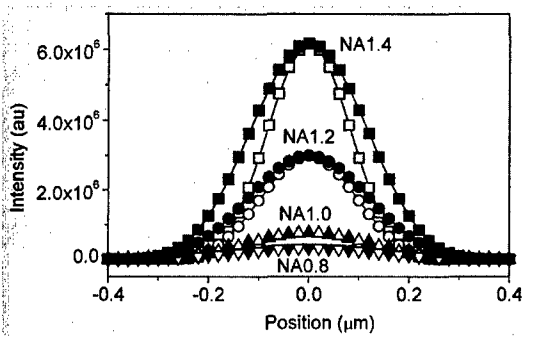

Figure 4. Two-photon point spread functions at focal plane. The open symbols denote the direction perpendicular to polarization (y axis) and solid symbols are within the polarization plane (x axis).

REFERENCES

1. S. Maruo, O. Nakamura and S. Kawata, Opt. Lett. **22**, 132 (1997).
2. S. Maruo and S. Kawata, J. IEEE MEMS **7**, 411 (1998).
3. H. –B. Sun, S. Matsuo and H. Misawa, Appl. Phys. Lett. **74**, 86 (1999).
4. B. H. Cumpston, S. P. Ananthavel, S. Barlow, D. L. Dyer, J. E. Ehrlich, L. L. Erskine, Ahmed A. Heikal, S. M. Kuebuler, I. -Y. Sandy Lee, D. M. Maugon, J. Qin, H. Rokel, M. Rumi, X. Wu, S. R. Marder and J. W. Perry, Nature 398, 51 (1999).
5. H. -B. Sun, T. Kawakami, Y. Xu, J.-Y. Ye, S. Matuso, H. Misawa, M. Miwa, and R. Kaneko, Opt. Lett. **25**, 1110 (2000).
6. H. -B. Sun, Y. Xu, S. Juodkazis, K. Sun, M. Watanabe, J. Nishii, S. Matsuo and H. Misawa, Opt. Lett. **26**, 325 (2001).
7. H. –B. Sun, V. Mizeikis, Y. Xu, S. Juodkazis, J. –Y. Ye, S. Matsuo and H. Misawa, Appl. Phys. Lett. 79, 1 (2001).
8. S. Kawata, H. –B. Sun, T. Tanaka and K. Takada, Nature 412, 667 (2001)
9. T. Tanaka, H. –B. Sun and S. Kawata, Appl. Phys. Lett. 80, 312 (2002).
10. K. D. Belfield, K. J. Schafer, Y. U. Liu, J. Liu, X. B. Ren and E. W. Van Stryland, J. Phys. Org. Chem, 13, 837 (2000).
11. H. –B. Sun, T. Tanaka, K. Takada and S. Kawata, Appl. Phys. Lett. 79, 1411 (2001).
12. H. –B. Sun, K. Takada and S. Kawata, Appl. Phys. Lett. 79, 3173 (2001).
13. H. -B. Sun, T. Tanaka and S. Kawata, Appl. Phys. Lett. 80, 3673 (2002)
14. H. –B. Sun, M. Maeda, K. Takada, J. Chon, M. Gu and S. Kawata, submitted.
15. M. Gu, Advanced Optical Imaging Theory (Springer, Heide lberg, 1999).

Tissue Engineering and Biomedical Applications